Available online at www.sciencedirect.com
SCIENCE DIRECT®
Pergamon
Cement and Concrete Research 33 (2003) 1047–1056
CEMENT AND CONCRETE RESEARCH

Rehydration and microstructure of cement paste after heating at temperatures up to 300 °C

M.C.R. Farage[a], J. Sercombe[b], C. Gallé[b,*]

[a]Conselho Nacional de Desenvolvimento Científico e Technológico, SEPN 507, Bloco B, Ed. Sede CNPQ 70740-901 Brasilia, DF, Brazil
[b]Direction de l'Energie Nucléaire, DPC/SCCME/LECBA, CEA-Centre de Saclay, Bat. 158, 91191 Gif-sur-Yvette Cedex, France

Received 4 April 2002; accepted 22 December 2002

Abstract

This paper is concerned with the evolution of the microstructure of cementitious materials subjected to high temperatures and subsequent resaturation in the particular context of long-term storage of radioactive wastes, where diffusive and convective properties are of primary importance. Experimental results obtained by mercury intrusion porosimetry (MIP) are presented concerning the evolution of the pore network of ordinary portland cement (OPC) paste heated at temperatures varying between 80 and 300 °C. The consequences of heating on the macroscopic properties of cement paste are evaluated by measures of the residual gas permeabilities, elastic moduli and Poisson's ratio, obtained by nondestructive methods. Resaturation by direct water absorption and water vapour sorption are used to estimate the reversibility of dehydration. The results provide some evidence of the self-healing capacity of resaturated cement paste after heating at temperatures up to 300 °C.

Keywords: Cement paste; Pore size distribution; Temperature; Mechanical properties; Adsorption

1. Introduction

Since the early 1950s the nuclear industry has generated radioactive wastes. The disposal and long-term management of these wastes is under study in many countries. As a general trend, the development of surface structures for the interim storage of high-level radioactive waste [1] or underground structures [2,3] for long-term storage, intermediate-level and possibly high-level waste are a focus of research activities. Cementitious materials are already widely used for waste conditioning and containers and could be further used for the formation of disposal engineering barriers [4,5]. For this reason, the French Atomic Energy Commission (CEA) has long been involved in research programs related to the long-term behaviour of cement-based materials [6–8]. The consequences of water immersion or flow (related to ground water) on cement microstructure and diffusive properties [6,9] have been of particular interest inasmuch as the main requirements concern the confinement of radionuclides.

Among the wastes intended for long-term underground storage, high-level wastes (spent fuel) are characterized by the important quantity of heat that they generate over decades. The surrounding structures may therefore be subjected to elevated temperatures (60–200 °C) over extended periods. Compared to the time scales considered for storage, these conditions will, however, only prevail for short periods and progressive water intrusion from the surroundings with temperature decay should eventually lead to complete resaturation of cementitious elements.

Many authors provide evidence that the loss of water, either free, adsorbed or chemically combined, induced by high temperatures, affects the microstructure of cement paste: capillary and total porosity increase [10–12] and the nanoporosity associated with C-S-H gel collapses [13,14]. In the temperature range 100–300 °C, these evolutions are mainly attributed to the loss of bound water from the C-S-H gel. Similar consequences have been reported for mortars and concretes [15–18], enhanced sometimes by the appearance of microcracks related to strain incompatibilities between the aggregates (which expand upon heating) and the cement paste (which shrinks upon heating). In comparison, very few data are available on the rehydration capacity

* Corresponding author. Tel.: +33-1-69-08-86-39; fax: +33-1-69-08-84-41.
E-mail address: galle@cea.fr (C. Gallé).

0008-8846/03/$ – see front matter © 2003 Elsevier Science Ltd. All rights reserved.
doi:10.1016/S0008-8846(03)00005-X

of cement paste and concrete [19] after exposure to elevated temperatures.

This paper presents experiments on the characterization of pore structure evolution of ordinary portland cement (OPC) with temperature. To this end, mercury intrusion porosimetry (MIP) tests have been performed on preheated cement paste samples and completed by measures of residual transport (gas permeabilities) and mechanical (elastic modulus, Poisson's ratio) properties. The rehydration capacity of cement paste was then studied by water absorption and water vapour adsorption tests.

2. Materials: characteristics, conditioning and sampling

The experimental program was carried out on neat cement paste made of French commercial CEM I 52.5 cement (OPC). Thirty cylindrical samples (40 mm in diameter and 80 mm high) were prepared with a water/cement ratio of 0.4 and kept at 100% humidity till demoulding at 24–48 h. The cylinders were sealed in plastic bags to avoid drying and kept at constant temperature (20 °C) for 7 years. These curing conditions are representative of storage site conditions, where external water supply will be limited during the first years after casting. Because of the requirements regarding each of the experimental techniques, three kinds of specimens were prepared: complete cylinders were directly used for gas permeability tests and ultrasonic testing, 10-mm-thick slices were cut off the cylinders to perform water absorption tests and 4 mm-thick-slices were used for MIP and vapour sorption tests. All the disks were taken from the middle part of the cylindrical samples (at least at 20 mm from the extremities) because lower and upper extremities tend to be slightly less and more porous than the middle part (a few percent).

3. Thermal treatments and experimental procedures

3.1. Thermal treatments

Thermal treatments were accomplished in a high-temperature Carbolite oven (maximum temperature of 600 °C, accuracy of control temperature ±1 °C). Drying temperatures were selected (1) to allow a comprehensive evaluation of the heating effects on the evolution of OPC microstructural properties and (2) to simulate the heat-exposure conditions prevailing in nuclear waste facilities. The chosen reference temperature was 80 °C, considered as a reference for the dried samples because heating at this temperature causes evaporation of free and adsorbed water with theoretically minimum C-S-H decomposition. Other reference temperatures were the following: 150 °C, the maximum temperature expected for underground storage of high-level wastes; 220 and 300 °C, temperatures at which pronounced decomposition of C-S-H occurs. In addition, most of the parameters were obtained on nonheated samples, stored at 20 °C, to characterize the reference state of the OPC paste.

Heating rates were limited at 0.1 °C/min to avoid thermal gradients and shocks. The thermal treatments were maintained until stabilization of mass loss was achieved, defined as less than 0.2% in 24 h. Temperature was then decreased at a similar rate of 0.1 °C/min until 60 °C. To control crack formation during the drying process, the external cylindrical surfaces of the probes were covered with at least two layers of self-adhesive aluminium paper. By uncovering the two ends of the probes, moisture gradients were vertically orientated, leading theoretically to vertical cracks. Once oven-dried, all the samples were stored in sealed plastic bags containing silica gel (to obtain a relative humidity [RH] close to 3%) to avoid any rehydration before testing.

3.2. Mercury intrusion porosimetry

MIP is commonly used to measure the mesopores and macropores of cement-based materials. A nonwetting fluid (mercury) is injected under successively higher increments of pressure into the porous material. The interpretation of test results is governed by the Washburn–Laplace equation in which the size of the pores (assumed to be cylindrical) are related to the applied pressure:

$$P = \frac{4\gamma\cos\theta}{d} \quad (1)$$

where P is the mercury injection pressure (Pa), γ is the surface tension of mercury (N/m), θ is the contact angle between solid and mercury (degrees), and d is the pore access diameter (m).

MIP tests were performed with a Micromeritics Autopore II 9220 mercury porosimeter with a (minimum) maximum injection pressure of (0.004) 413 MPa. Between two and five samples were used for each temperature level, obtained from the center part of the 4-mm-thick slices.

It is well known that MIP does not give a complete and exact representation of the pore structure [20,21]. Because mercury must pass through the narrowest pores connecting the pore network before entering the samples, large pores accessible through narrow necks can be recorded as small pores. Because of the high mercury pressures used to access fine pores, C-S-H gel can collapse and therefore lead to an incorrect estimation of pore volume. Nevertheless, MIP remains a powerful tool mainly for comparative analysis of hydrated cements of various ages and w:c ratios [20], or subjected to different external conditions [22].

3.3. Mechanical properties

The elastic modulus (E) and Poisson's ratio (ν) were determined by nondestructive techniques. The equipment consists of an ultrasonic testing system (MATEC Instru-

ments) that generates a pulse of vibration at an ultrasonic frequency, transmitted to the sample by a first transducer and received after passing through the sample by a second transducer. The equipment measures propagation times of both shear waves (S waves) and longitudinal waves (P waves). By considering the material as isotropic and homogeneous, the mechanical properties of cement paste can be obtained according to the following constitutive relations [23]:

$$E = \rho \frac{V_s^2(3V_p^2 - 4V_s^2)}{V_p^2 - V_s^2} \quad (2)$$

$$\nu = \frac{0.5(V_p/V_s)^2}{(V_p/V_s) - 1} \quad (3)$$

where ρ is the material density (kg/m^3) and V_s and V_p are the shear and longitudinal wave velocities (m/s), respectively. E is obtained in pascals. At least three complete cylindrical samples were tested for each temperature level.

3.4. Gas permeability

Gas permeability measures were obtained with a Hassler apparatus, shown in Fig. 1. This device is a constant-head permeameter type [24], specially adapted to inject dry nitrogen through laterally confined cylindrical samples of cement paste with a diameter of 40 mm and a height varying between 40 and 80 mm. Gas flow rates are measured with bubble flowmeters. Effective gas permeability (k_g, in square meters) are calculated with Darcy's law as modified by the Hagen–Poiseuille relation:

$$k_g = \frac{2QLP_2\mu}{S(P_1^2 - P_2^2)} \quad (4)$$

where Q is the gas flow rate measured at pressure P_2 (m^3/s); L and S are the specimen height (m) and cross section (m^2), respectively; μ is the dynamic viscosity of the gas, P_1 is the absolute injection pressure (Pa) and P_2 is the exit pressure.

Intrinsic permeabilities k (m^2) are determined using the Klinkenberg approach [25], which proved to be adequate for cementitious materials [17,26]. In this method, the intrinsic permeability is obtained from measures of the effective permeability performed at different pressures, according to the following relation:

$$k_g = k\left(1 + \frac{\beta}{(P_1 + P_2)/2}\right) \quad (5)$$

in which β is the Klinkenberg constant. To avoid potential damage of the samples during the permeability tests, the confinement pressure was limited to 1 MPa and the injection pressures (P_1) did not exceed 1.4 MPa. Three samples were tested at each temperature.

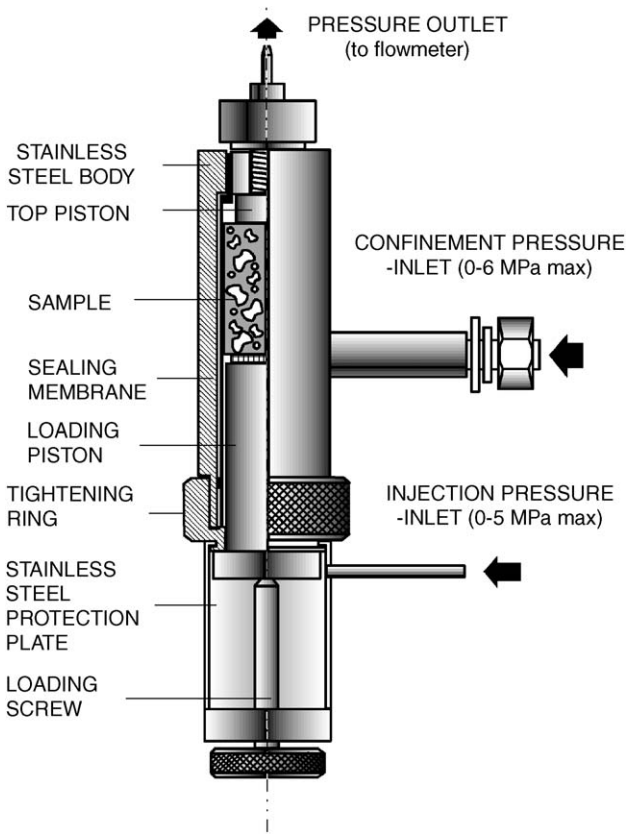

Fig. 1. Scheme of the Hassler gas permeameter.

4. Resaturation techniques

4.1. Water absorption

Resaturation of the samples was first performed by water absorption. After oven-drying at 80, 150, 220 or 300 °C, samples 10 mm thick (three per temperature) were used: the disks were resaturated under water at 20 °C in a closed chamber, the air space of which was previously evacuated. To estimate the total pore volume, the samples were dried again at 80 °C until mass loss stabilized. Total porosity is given as a function of the mass of lost water (Δm=($m_{sat} - m_{dry}$)) according to the following expression:

$$\phi = \frac{m_{sat} - m_{dry}}{V\rho_w} \quad (6)$$

where m_{dry} and m_{sat} are the mass of the samples after and before the second drying at 80 °C, respectively; V is the sample volume (m^3); and ρ_w is the water density (kg/m^3) at 20 °C.

4.2. Vapour sorption

The water vapour adsorption experiments provided more realistic conditions with respect to underground storage site

Table 1
Salt solutions and related RHs

RH (T=80 °C)	10%	26%	35%	51%	65%	74%	96%
Salt solution	LiCl	$MgCl_2$	K_2CO_3	NaBr	$NaNO_3$	NaCl	K_2SO_4

conditions and are nondamaging means of resaturating the samples. The tests were performed using the saturated solution method [27] at a constant temperature of 80 °C. The temperature was chosen mainly to accelerate the tests. Specimens were suspended in sealed desiccators where the RH was controlled by saturated salt solutions, as indicated in Table 1.

Cement paste disks 4 mm thick were used for the experiments. After oven-drying at the different temperature levels (80 to 300 °C), the specimens (three per temperature) were submitted to a step-by-step adsorption at 80 °C, each step being maintained till stabilization of mass (mass variations less than 2% in 7 days). The corresponding water content (per mass of dry specimen) at each RH was determined by mass changes. Once the adsorption isotherms were complete (mass stabilization at 96% humidity), the samples were oven-dried again at 80 °C to estimate the total free water content.

5. State of cement paste after heating

5.1. Mass loss

The state of the samples after thermal heating was found to depend on two factors: the maximum temperature reached and the thickness of the specimen (4, 10 or 80 mm). Increasing temperatures led to increasing cracking of the complete cylindrical samples. As expected, drying-induced cracks were, however, vertically orientated, starting from the lower and upper unprotected surfaces of the complete specimen. Removal of these end parts led to visually uncracked samples. Owing to their reduced size, no cracks were observed on the 4-mm-thick disks after heating. Fig. 2 presents the effect of temperature on mass loss.

Overall, the relative mass variation, $m_0 - m_{dry}/m_0$ (with m_0 as the initial mass of the samples), was found proportional to the treatment temperature. The dispersion of data may be attributed to the varying duration of hydrothermal conditions taking place during heating, which depend mainly on the size and shape of the samples [28] (the rate of heating and sealing conditions being identical for all the samples). The temperature range 100–300 °C is in fact the most favourable for the formation of internal autoclaving conditions in cement paste, leading to additional hydration of unhydrated cement grains [12]. This could explain the general tendency, observed in Fig. 2, of the bound water content, as revealed by mass loss, to increase as the thickness of the samples decreased.

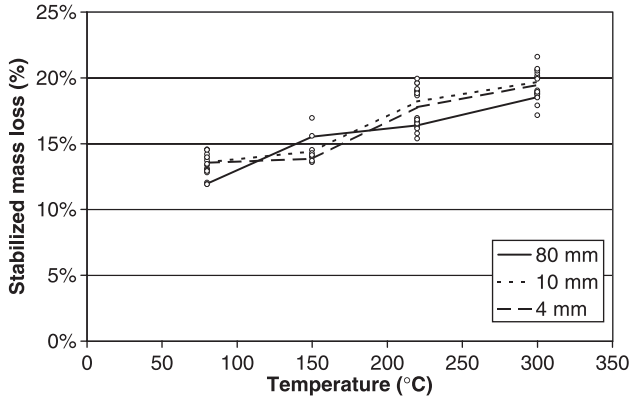

Fig. 2. Stabilized mass loss as a function of the temperature of the thermal treatment for samples of different thicknesses.

For temperatures up to 80 °C, evaporable moisture plays a dominant role. Adsorbed water is known to remain stable for temperatures not exceeding 65–80 °C [29,30]. It is furthermore generally accepted that the hydration products of OPC remain chemically unaltered within this temperature range [31,32]. For higher temperatures, moisture loss results either from the escape of interlayer water from the C-S-H gel (90–105 °C [29]) or loss of bound water. The former is known to be completely reversible, but little is known concerning the reversibility of the latter.

5.2. Mercury intrusion pore size distribution

The initial pore structure of the paste was investigated at first by MIP tests. Water from the samples was removed by freeze-drying. Differential intrusion curves are presented in Fig. 3.

For OPC pastes, the main classes of pores usually encountered in MIP depend on the degree of hydration of the material, and hence on the w:c ratio and curing conditions. The curves of Fig. 3, where two main peaks appear, are characteristic of a partially hydrated cement paste [20]. The first sharp "initial peak," having pore access diameters around 0.3–0.5 μm, corresponds to the minimum dimension

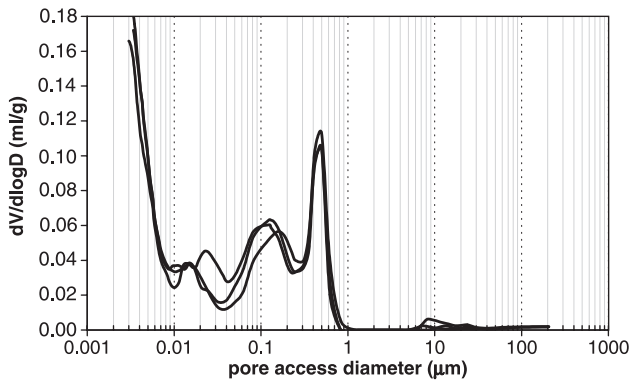

Fig. 3. Pore size distribution of freeze-dried cement paste.

of an interconnected (to the surface) capillary network (it defines the so-called "threshold diameter" [21]), which normally reduces as hydration proceeds and hydration products fill the pore space [20]. The second rounded peak (at pore access diameters around 0.02–0.2 μm), rather than being related to a given pore size, has been attributed to the crushing strength of the gel [20]—it corresponds to the pressure required to break through blockages in the capillary pore network—which occurs here for mercury pressures between 6 and 30 MPa.

MIP curves of Fig. 3 reveal therefore the poorly hydrated initial state of the cement paste. This most probably originates from the low w:c ratio of the paste (0.4) compared to that theoretically required for complete hydration under sealed conditions (0.44) [33].

Differential intrusion curves for the samples heated at 80, 150, 220 and 300 °C are presented in Fig. 4. All the curves show similar patterns with respect to that of the freeze-dried specimen (20 °C). The two previously defined peaks are clearly apparent, located at pore access diameters apparently slightly shifted towards smaller diameters. Table 2 presents the evolution of the total mercury porosity (%) and of the porosity (%) associated with the second rounded peak (pore access diameters in the range 0.02–0.2 μm), together with the threshold diameter corresponding to the first peak.

The total mercury porosity changed mainly between 20 and 150 °C (+12%) and remained almost stable for higher temperatures. This variation is, however, small when compared to that associated with the second rounded peak (0.02–0.2 μm) which shows a marked increase between 20 and 80 °C (+50%). This indicates that major changes in the microstructure of cement paste take place at temperatures as low as 80–150 °C. The origin of these changes could be the loss of interlayer water from the C-S-H gel, resulting in the collapse of part of its microstructure. As shown also in Ref. [12], the consequences on MIP curves are twofold: increasing volume of injected mercury in the gel crushing region (0.02–0.2 μm) and decreasing volume of injected mercury for higher mercury pressures (e.g., for micropores associated with C-S-H gel with pore access diameters less than 0.02 μm). Similar conclusions were obtained recently on heated concrete specimen [17]. The threshold diameter, being characteristic of a capillary network connected to the surface of the samples, showed no variation with temperature.

Table 2
Porosity and threshold diameter obtained by MIP

Temperature (°C)	Threshold diameter (μm)	Second peak porosity (%)	Total porosity (%)
20	0.5	6.8	21.0
80	0.2	10.2	21.8
150	0.4	9.4	24.0
220	0.6	11.2	23.8
300	0.4	12.0	23.7

5.3. Elastic modulus and Poisson's ratio

The evolution of cement paste macroscopic properties can also give some information on its microstructure. Mathematical models relating cement paste mechanical characteristics (elastic modulus, compressive strength) and porosity have been proposed [30,34,35], based on extensive surveys. They will be used hereafter to investigate the evolution of total porosity with temperature. Figs. 5 and 6 present test results on the elastic modulus and Poisson's ratio of cement paste as a function of temperature, respectively.

Compared with the elastic modulus of concrete, which usually decreases by a factor of 2 between 20 and 250 °C [17,36], the elastic modulus of OPC paste heated at 300 °C lost only 17% with respect to its initial value. Major evolutions occurred between 20 and 80 °C (−8%), probably related to removal of free and adsorbed water. The sensitivity of the test methods, which become rapidly useless if significant cracking occurs, demonstrates that thermal damage remained limited. The changes can therefore be attributed mainly to modifications of the internal microstructure of cement paste. The test results of Fig. 6, on

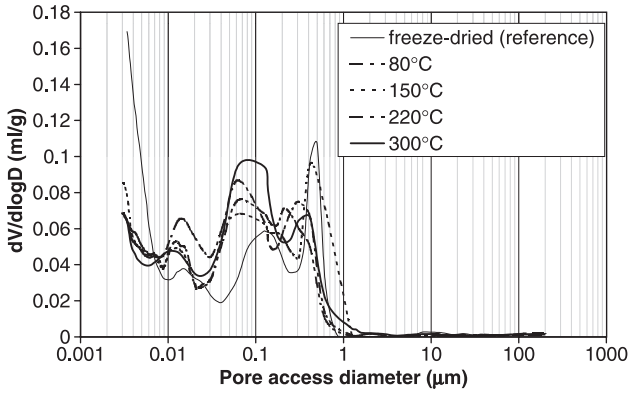

Fig. 4. Pore size distribution of thermally treated cement paste.

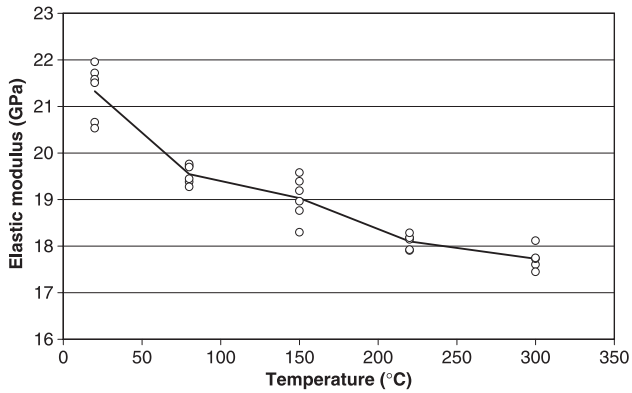

Fig. 5. Evolution of the elastic modulus of cement paste with temperature.

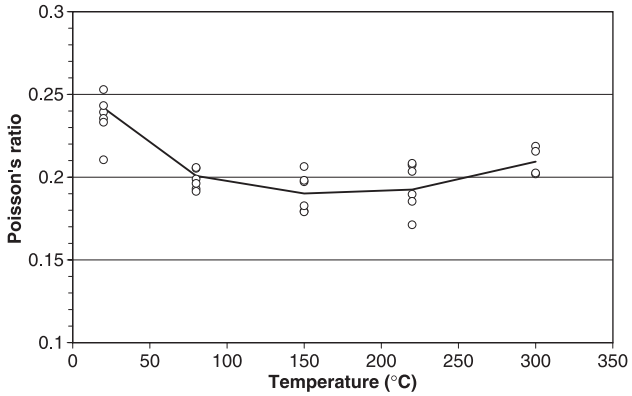

Fig. 6. Evolution of the Poisson's ratio of cement paste with temperature.

Poisson's ratio, confirmed that major changes occurred at temperatures as low as 80 °C.

5.4. Intrinsic permeability

The nitrogen permeability measurements were performed twice on the same samples, before and after removal of the cracked extremities (5 mm on each side). The aim of the second data set was to estimate the impact of highly cracked sections on the results. Experimental data showing the effective gas permeability, k_g, as a function of the inverse of the mean pressure, $P=(P_1+P_2)=2$ [Eq. (5)] are given in Fig. 7 for each temperature.

As expected from the Klinkenberg approach [Eq. (5)], increasing pressures lead to smaller effective permeabilities, showing the good mechanical state of the samples: damaged specimens tend to give increased permeability when subjected to increasing pressures. As a rule, the data presented little dispersion. After heating at 300 °C, results showed slightly more spread, which could be a consequence of the more pronounced cracking of the samples. As shown in Fig. 7, the two series (with and without cracked ends) did not differ significantly in effective gas permeabilities: linear regression was used to estimate the intrinsic permeabilities.

Table 3
Intrinsic permeability of cement paste as a function of temperature

Temperature (°C)	First series, intrinsic permeability (10^{-16} m^2)	Second series, intrinsic permeability (10^{-16} m^2)
80	1.5	1.5
150	0.5	1.0
220	1.4	1.7
300	1.8	1.8

As indicated by the results of the two test series (Table 3), the intrinsic permeability did not vary significantly with the temperature of the thermal treatment. MIP investigations on samples analyzed before and after permeability tests revealed that the microstructure of cement paste was considerably modified during the tests, as shown in Fig. 8. Particularly, the volume of injected mercury between pore access diameters (0.02–0.2 μm) corresponding to the second rounded peak, increased significantly during the tests. The curves of Fig. 8 also show that the effect of gas injection are similar for samples heated previously at 80 and 220 °C, and far more important than the differences

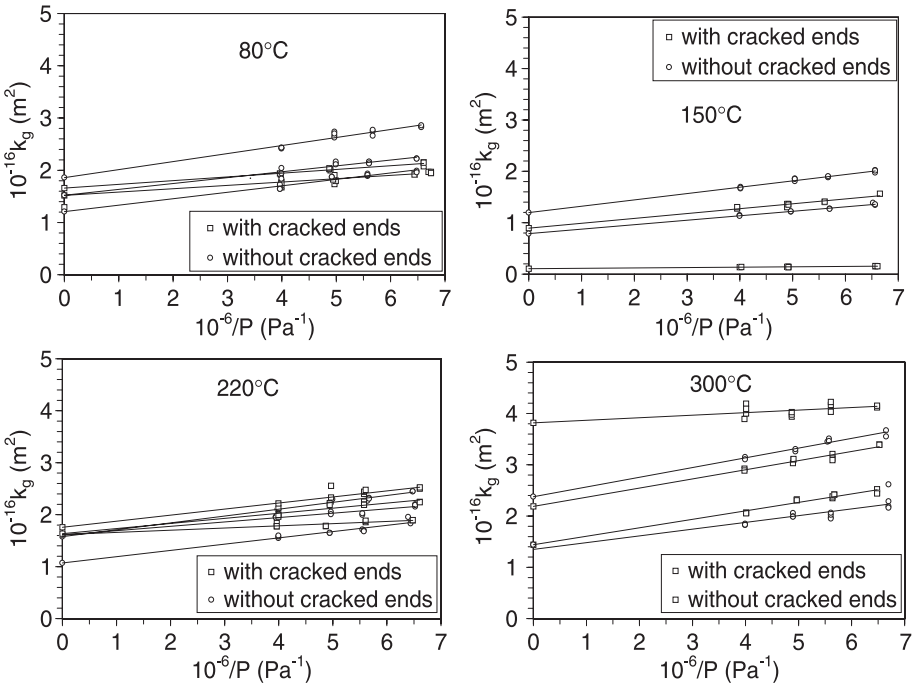

Fig. 7. Evolution of the effective gas permeability as a function of the inverse of the mean pressure for different temperatures.

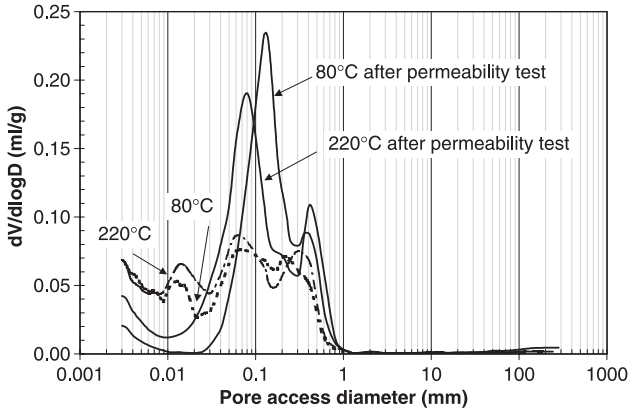

Fig. 8. Impact of gas permeability tests on the microstructure of heated cement paste.

arising because of thermal treatment. This could explain the lack of variation of the intrinsic permeabilities with temperature (Table 3).

6. State of cement paste after resaturation

6.1. Total porosity

The stabilized mass variations (in percent of the dry mass of the samples after first heating at 80, 150, 220 or 300 °C), obtained after the vacuum resaturation and subsequent drying at 80 °C, are represented by the curves of Fig. 9, based on average experimental values. Resaturation led to increasing gain of water with increasing temperatures. Part of this water was retained upon subsequent drying at 80 °C, showing that some of it had been combined by rehydration or hydration of previously unhydrated cement. This phenomenon did not occur for the samples preheated at 80 °C (the water gain and loss were found to be identical).

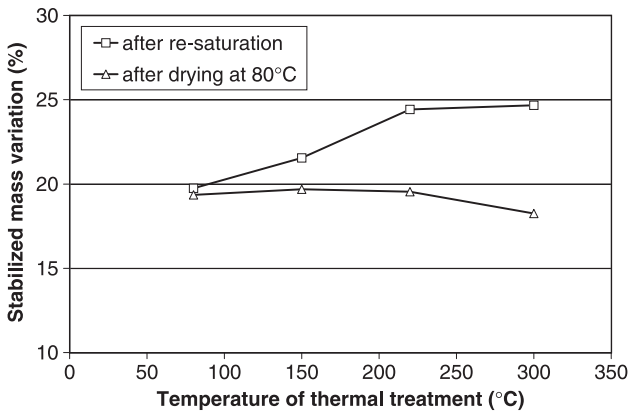

Fig. 9. Stabilized mass variations after resaturation and subsequent drying at 80 °C of the samples as a function of the temperature of the thermal treatment.

Calculations of the total porosity of the cement paste after resaturation, according to Eq. (6), led to the curve "after resaturation" (Fig. 10). Obviously, preheated samples at temperatures more than 80 °C recovered their initial total porosity (32.5% for the samples heated at 80 °C), with even a slight improvement owing to hydration (29% for the samples preheated at 300 °C). To quantitatively estimate the total porosity of the cement paste before resaturation and compare it to the latter, the measures of residual elastic moduli were used. It has been shown that the elastic modulus of cement paste may be calculated as a function of the material porosity ϕ (total or capillary porosity) by the following expression [30,35]:

$$E = E_{sk}(1-\phi)^3 \tag{7}$$

where E_{sk} is the elastic modulus of the solid skeleton (with zero porosity). To estimate the skeleton modulus (E_{sk} = 63.7 GPa), the total porosity (32.5%) and the elastic modulus (19.5 GPa) of the samples preheated at 80 °C were used in Eq. (7). The curve "before resaturation" of Fig. 10 gives the estimation of total porosity evolutions with temperature, as obtained from the residual elastic moduli. The variation between 20 and 300 °C is small (+13.6%) but consistent with mercury porosimetry measurement (+12.8%). The trend (increasing porosity for higher treatment temperature) is opposite to that obtained after the resaturation of the samples. This confirms that partial rehydration of the cement paste took place during the resaturation phase.

6.2. Water vapour adsorption isotherms

Water vapour adsorption isotherms obtained for the samples preheated at the four temperatures (80, 150, 220, 300 °C) are plotted in Fig. 11. Water contents are expressed (in %) per unit mass of dry cement paste. Each point is the mean value obtained from three samples. All the adsorption isotherms were obtained at a constant temperature of 80 °C. The shape of the curves are typical for cementitious materials [27],

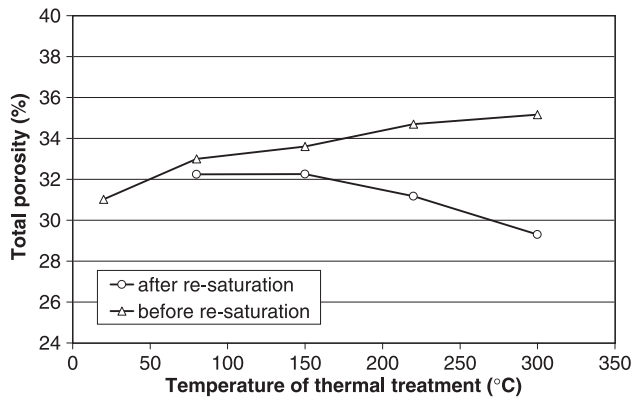

Fig. 10. Evolution of the total porosity of cement paste before and after resaturation as a function of the temperature of thermal treatment.

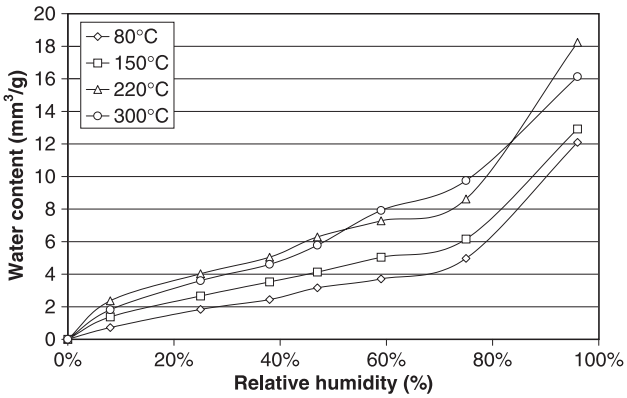

Fig. 11. Water vapour adsorption isotherms for the preheated cement paste samples.

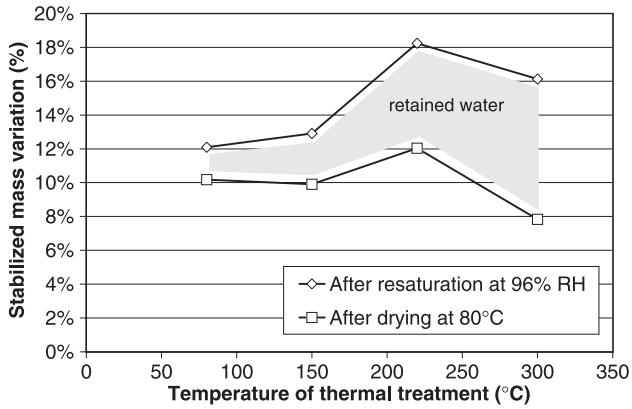

Fig. 12. Stabilized mass variations for the samples after resaturation at 96% RH and subsequent drying at 80 °C as function of the temperature of the thermal treatment.

showing a rapid initial increase of moisture content followed by a nearly constant slope in the RH range 40–75%.

Overall, the water content evolutions of Fig. 11 gave similar results to those obtained from the vacuum resaturation curves of Fig. 9. At each datum, the quantity of "adsorbed water" increased with the temperature of the thermal treatment. However, analysis and interpretation of the isotherms leads to important differences. The moisture contents obtained for relative humidities less than or in the range 40–75% are significantly increased by temperature: the samples preheated at 150, 220 and 300 °C before sorption tests gain 50%, 75% and 100% more water, respectively, than those preheated at 80 °C. Compared with the results obtained after complete water resaturation (see Fig. 9), where the samples preheated at 300 °C took only 25% more water than those preheated at 80 °C, it is shown that major differences in water gain occurred at small to medium RH.

These results are of importance because it is generally considered that the low-pressure part of the water vapour adsorption curves varies little with the w:c ratio, being closely related to the C-S-H gel content [27,33]. In the present study, the origin of resaturation at low to medium vapour pressures may be attributed to:

- physical adsorption in multimolecular layers on the pore surface of the C-S-H gel, according to the well-known BET theory originally proposed by Brunauer et al. [37],
- reentry of water molecules into vacant interlayer spaces, as shown by Feldman and Ramachandran [29],
- partial hydration of unhydrated cement grains in view of the initially poorly hydrated state of the cement paste,
- rehydration of decomposed C-S-H gel products.

In principle, the adsorption isotherms determined by BET [27] may be used to determine specific surface areas. BET surface is closely related to the internal surface of C-S-H gel, which comprises most of the internal surface of cement paste. The probable partial rehydration of the cement paste samples and reentry of interlayer water renders the technique only partially applicable. At least, the effect of preheating on moisture gain, whatever its origin, can be assessed by this way. Specific surface areas (in m^2/g of dry cement paste) and BET constant obtained for the tested cement paste samples are presented in Table 4 and compared to that measured by MIP.

As shown in Table 4, the higher the preheating temperature, the higher the specific surface area. In comparison, the specific surface area of capillary pores, as measured by MIP, remained almost constant for temperatures exceeding 80 °C. This indicates again that the differences originate mainly from C-S-H internal microstructure or/and (re)hydration of unhydrated cement particles. The latter would be consistent with increasing BET parameters, which is characteristic of the water/pore interactions. Complete drying of the samples at 80 °C after completion of the adsorption tests (at 96% RH) confirmed that a significant part of the adsorbed water was retained within the cement paste (see Fig. 12).

Table 4
Specific surface areas S_s and BET constant, as determined from experimental data by the BET method and MIP

Temperature (°C)	S_s BET (m^2/g)	S_s MIP (m^2/g)	BET constant
80	68	29	6
150	86	30	12
220	113	31	13
300	118	28	22

7. Conclusions

The results of the experimental investigations performed on the cement paste samples after heating at temperatures in the range 80–300 °C revealed that:

1. The cement paste used in MIP analyses was initially only partially hydrated. Consequently, the pore size distribution was characterized by two main peaks associated with

a capillary network connected to the surface of the samples (sharp peak with "threshold diameters" around 0.2–0.6 μm) and with the crushing strength of C-S-H gel (rounded peak for pore access diameters in the range 0.02–0.2 μm). Upon heating, no additional peak appeared. The increase of total injected mercury volume with temperature (+12% at 300 °C) originated mainly from the increase of injected mercury volume related to the rounded peak (pore access diameters in the range 0.02–02 μm). The latter can be attributed to the collapse of C-S-H gel microstructure upon heating, which occurs mainly for temperatures between 80 and 150 °C. These results are consistent with that obtained on well-hydrated samples by other authors [12–14].

2. Mechanical properties (elastic modulus, Poisson's ratio) decreased slightly (−17% at 300 °C) with temperature. In magnitude, the evolution was consistent with total mercury porosity changes as measured by MIP.

3. Transport properties (nitrogen permeabilities) after heating were independent of temperature. Further MIP analyses revealed that the percolation of nitrogen under low pressures (4 bar) during the tests led to an important increase of mercury porosity, which can explain this lack of variation.

4. After resaturation by water absorption or water vapour adsorption, the cement paste samples heated at temperatures up to 300 °C recovered their original total porosity, comparable to that measured after a heating treatment at 80 °C. This shows that some degree of reversibility exist for OPC pastes heated at temperatures up to 300 °C, originating from rehydration of decomposed C-S-H or hydration of initially unhydrated cement grains.

References

[1] A. Lioure, B. Porzio, P. Jaecki, C. Moitrier, I. Tirel, C. Villard, C. Leroy, A. Marvy, D. Iracane, Long-term interim storage of thermal HLW: importance, constraints and principles for the management of long times in storage, International Conference GLOBAL2001, Paris, 2001.

[2] J.L. Gaussen, Bure's underground research laboratory: general framework, objectives, siting process and schedule of the URL project, International Conference GLOBAL2001, Paris, 2001.

[3] M.L. Matthews, Progress in long-lived radioactive waste management and disposal at the waste isolation pilot plant, International Conference GLOBAL2001, Paris, 2001.

[4] F.P. Glasser, M. Atkins, Cements in radioactive waste disposal, MRS Bull. (1994, December) 33–38.

[5] C.R. Wilding, The performance of cement based systems, Cem. Concr. Res. 22 (2) (1992) 299–310.

[6] F. Adenot, M. Buil, Modelling of corrosion of cement paste by deionized water, Cem. Concr. Res. 22 (3) (1992) 489–495.

[7] F. Adenot, C. Richet, P. Faucon, Long-term prediction of concrete durability in radioactive waste management: influence of the pH of the aggressive solution, in: A. Al-Manaseer, S. Nagataki, R.C. Joshi (Eds.), International Conference on Engineering Materials, Ottawa, Proc. Int. Conf. on Eng. Mat., vol. 2, 1997, pp. 107–113.

[8] M. Mainguy, C. Tognazzi, J.M. Torrenti, F. Adenot, Modelling of leaching in pure cement paste and mortar, Cem. Concr. Res. 30 (1) (2000) 83–90.

[9] C. Richet, Etude de la migration des radioéléments dans les liants hydrauliques—influence du vieillissement des liants sur les mécanismes et la cinétique des transferts, Doctoral thesis, University of Paris XI, 1992.

[10] R. Fisher, On the behavior of cement mortar and concrete at high temperatures, Deutscher Ausschus für Stahlbeton, Ernst and Sohn, Berlin, 1970.

[11] T.Z. Harmathy, Thermal properties of concrete at elevated temperatures, ASTM J. Mater. 1 (5) (1970) 47–74.

[12] J. Piasta, Z. Sawicz, L. Rudzinski, Changes in the structure of hardened paste due to high temperature, Mater. Struct. 100 (1984) 291–296.

[13] U. Diederichs, K. Hinrichsmeyer, U. Schneider, Analysis of thermal, hydrothermal and mechanical stresses of concrete by mercury porosimetry and nitrogen sorption, RILEM/CNR Symposium on Principles and Applications of Pore Structural Characterization, Milano, Italy, 1983, pp. 409–427.

[14] U.M. Jumppanen, U.M. Diederichs, K. Hinrichsmeyer, Material properties of F-concrete at high temperatures, Technical Report 542, Espoo Research Centre, Finland, 1986.

[15] F.S. Rostasy, R. Weiss, G. Wiedemann, Changes of pore structure of cement mortars due to temperature, Cem. Concr. Res. 10 (1980) 157–164.

[16] F.S. Rostasy, K. Hinrichsmeyer, Structural alterations in concrete due to thermal and mechanical stresses, First International Conference on Materials Science to Construction Materials Engineering, Versailles, France, 1987.

[17] C. Gallé, J. Sercombe, Permeability and pore structure evolution of silico-calcareous and hematite high-strength concretes submitted to high temperatures, Mater. Struct. 34 (2001) 619–628.

[18] M. Tsimbrovska, P. Kalifa, D. Quénard, J.F. Daian, High-performance concrete at elevated temperature: permeability and microstructure, in: F. Livolant (Ed.), International Conference SMIRT 14, Lyon, France, 1997, pp. 475–482.

[19] W.M. Lin, T.D. Lin, L.J. Powers-Couche, Microstructures of fire-damaged concrete, ACI Mater. J. 93 (3) (1996) 199–205.

[20] R.A. Cook, K.C. Hover, Mercury porosimetry of hardened cement pastes, Cem. Concr. Res. 29 (1999) 933–943.

[21] S. Diamond, Mercury porosimetry. An inappropriate method for the measurement of pore size distributions in cement-based materials, Cem. Concr. Res. 30 (2000) 1517–1525.

[22] C. Gallé, Effect of drying on cement-based materials pore structure as identified by mercury intrusion porosimetry. A comparative study between oven-, vacuum-, and freeze-drying, Cem. Concr. Res. 31 (2001) 1467–1477.

[23] T. Bourbié, O. Coussy, B. Zinszner, Acoustique des milieux poreux, Publications de l'IFP, Collection Science et Technique du pétrole, vol. 27, 1986.

[24] C. Gallé, J.F. Daian, Gas permeability of unsaturated cement-based materials: application of a multi-scale network model, Mag. Concr. Res. 52 (4) (2000) 251–263.

[25] L.J. Klinkenberg, The permeability of porous media to liquids and gases, API Drill. Prod. Pract. (1941) 200–213.

[26] D. Perraton, La perméabilité au gaz du béton, Doctoral thesis, INSA, Toulouse, France, 1992.

[27] V. Baroghel-Bouny, Caractérisation des pâtes de ciment et des bétons. Méthodes, analyse, interprétations, LCPC Publications, Paris, France, 1994.

[28] G.A. Khoury, Compressive strength of concrete at high temperatures: a re-assessment, Mag. Concr. Res. 161 (44) (1992) 291–309.

[29] R.F. Feldman, V.S. Ramachandran, Differentiation of interlayer and adsorbed water in hydrated Portland cement by thermal analysis, Cem. Concr. Res. 1 (1971) 607–620.

[30] H.F.W. Taylor, Cement Chemistry, 2nd ed., Thomas Telford, London, 1997.

[31] G. Verbeck, R. Helmuth, Structures and physical properties of cement paste, Fifth International Symposium on the Chemistry of Cement, Tokyo, China, 1968, pp. 1–32.

[32] G. Verbeck, L.E. Copeland, Some physical and chemical aspects of high-pressure steam-curing, Menzel Symposium on High-Pressure Steam-Curing, ACI SP-32, Detroit, 1972, pp. 1–13.
[33] T.C. Powers, T.L. Brownyard, Studies of the physical properties of hardened Portland cement paste, J. Am. Concr. Inst. 22 (9) (1947) 971–992.
[34] J.J. Beaudoin, R.F. Feldman, P.J. Tumidajski, Pore structure of hardened Portland cement pastes and its influence on properties, Adv. Cem. Based Mater. 1 (1994) 224–236.
[35] K. Kendall, A.J. Howard, J.D. Birchall, The relation between porosity, microstructure and strength, and the approach to cement-based materials, Philos. Trans. R. Soc. Lond., A 310 (1983) 139–153.
[36] Z.P. Bazant, M.F. Kaplan, Concrete at high temperatures, Material Properties and Mathematical Models, Longman House, Burnt Mill, UK, 1996.
[37] S. Brunauer, P.H. Emmett, E.J. Teller, Adsorption of gases in multimolecular layers, J. Am. Chem. Soc. 60 (1938) 309–319.